AIP Advances

RESEARCH ARTICLE | DECEMBER 08 2023

On the identifiability and statistical features of a new distributional approach with reliability applications

Badr Alnssyan ; Zubair Ahmad ; Jean-Claude Malela-Majika ; Jin-Taek Seong ; Wasswa Shafik

AIP Advances 13, 125211 (2023)
https://doi.org/10.1063/5.0178555

On the identifiability and statistical features of a new distributional approach with reliability applications

Cite as: AIP Advances 13, 125211 (2023); doi: 10.1063/5.0178555
Submitted: 27 September 2023 • Accepted: 13 November 2023 •
Published Online: 8 December 2023

Badr Alnssyan,[1,a] Zubair Ahmad,[2,b] Jean-Claude Malela-Majika,[3,c] Jin-Taek Seong,[4,d] and Wasswa Shafik[5,d]

AFFILIATIONS

[1] Unit of Scientific Research, Applied College, Qassim University, Buraydah 51452, Saudi Arabia
[2] Department of Statistics, Quaid-i-Azam University, Islamabad 44000, Pakistan
[3] Department of Statistics, Faculty of Natural and Agricultural Sciences, University of Pretoria, Hatfield, 0028 Pretoria, South Africa
[4] Graduate School of Data Science, Chonnam National University, Gwangju 61186, Republic of Korea
[5] Dig Connectivity Research Laboratory (DCRLab), Ndejje University, P.O. Box 600040, Kampala, Uganda

[a] b.alnssyan@qu.edu.sa
[b] z.ferry21@gmail.com
[c] malela.mjc@up.ac.za
[d] **Authors to whom correspondence should be addressed:** jtseong@jnu.ac.kr and asswashafik@dcrlab.org

ABSTRACT

Probability distributions have prominent applications in different sectors. Among these sectors, probability models are mostly used to analyze datasets in engineering. Among the existing probability distributions, the two-parameter Weibull model plays an important role in providing the best fit for engineering and other related datasets. This paper introduces a new method called a novel updated-*W* (denoted by "NU-*W*") family of distributions that is used to develop a new updated form of the Weibull distribution. The proposed updated extension of the Weibull model is referred to as a novel updated Weibull (denoted as NU-Weibull) distribution. Distributional properties such as identifiability, heavy-tailed characteristic, and *r*th moment of the NU-*W* family are derived. The residual life analysis of the NU-Weibull distribution is provided. Finally, two physical applications from civil engineering and reliability sectors are analyzed to demonstrate the application and effectiveness of the NU-Weibull distribution. The data fitting results show that the NU-Weibull distribution is a more suitable and best fit for engineering datasets.

I. INTRODUCTION

In most real-life scenarios, probability distributions are often adopted and implemented for data modeling in various situations. In the middle of them, the Weibull-type distribution is often used to model engineering-related datasets; see Ref. 1.

The two-parameter Weibull distribution is greatly used in applied sciences, particularly in engineering-related fields. The fruitful implementations of the Weibull distribution in engineering include the following engineering fields: (i) wind energy; see Ref. 2, (ii) civil engineering; see Ref. 3, (iii) reliability engineering; see Ref. 4, (iv) industrial engineering; see Ref. 5, (v) mechanical engineering; see Ref. 6, and (vi) electrical engineering; see Ref. 7.

Assume the random variable T has the Weibull distribution with CDF (cumulative distribution function) $W(t;\psi)$ defined by

$$W(t;\psi) = 1 - e^{-\sigma t^{\eta}}, \quad t \geq 0, \sigma > 0, \eta > 0, \tag{1}$$

where $\psi = (\eta, \sigma)$.

Corresponding to $W(t;\psi)$ in Eq. (1), the PDF (probability density function) symbolized by $w(t;\psi)$, HF (hazard function) symbolized by $h(t;\psi)$, SF (survival function) symbolized by $S(t;\psi)$, and CHF (cumulative hazard function) symbolized by $H(t;\psi)$ are expressed by

$$w(t;\psi) = \eta\sigma t^{\eta-1} e^{-\sigma t^{\eta}},$$

$$h(t;\psi) = \eta\sigma t^{\eta-1},$$

$$S(t;\psi) = e^{-\sigma t^{\eta}},$$

and

$$H(t;\psi) = -\log\left(1 - e^{-\sigma t^{\eta}}\right),$$

respectively.

From $h(t;\psi)$, it is easily detectable that the HF of the Weibull distribution has three possible behaviors. The three behaviors of $h(t;\psi)$ include (a) constant when $\eta = 1$, (b) increasing for $\eta > 1$, and (c) decreasing when $\eta < 1$.

In many sectors, especially in the engineering sector, the behavior (or hazard function) of the datasets changes over time non-monotonically. In such scenarios, the selection of the Weibull distribution for conducting data analysis is not a sensible choice to implement; see Ref. 8.

To enhance and improve the fitting power and distributional flexibility, various updated forms of the Weibull distribution with different behaviors of $h(t;\psi)$ have been introduced; see, for instance, the following Weibull-type distributions: (i) new inverse Weibull (NI-Weibull) distribution; see Ref. 9, (ii) odd lomax-G inverse Weibull (OLGI-Weibull) distribution; see Ref. 10, (iii) truncated translated Weibull (TTWeibull) distribution; see Ref. 11, (iv) bimodal Weibull (B-Weibull) distribution; see Ref. 12, (v) Pareto-Weibull (P-Weibull) distribution; see Ref. 13, (vi) new extended Weibull (NEx-Weibull) distribution; see Ref. 14, and (vii) discrete Weibull (D-Weibull) distribution; see Ref. 15, and for more details, see Refs. 16–27.

In this paper, we provide a new useful, modified, and improved version of the Weibull distribution. The new improved version of the Weibull distribution is introduced based on a new probabilistic approach called the novel update-W (NU-W) method or family. The newly amended version of the Weibull distribution can be called a novel updated Weibull (NU-Weibull) distribution. With the help of the NU-W method, new amended versions of other distributions can also be introduced.[28]

This paper is subdivided (or structured) into numerous subsections, for instance, in Sec. II, the NU-W family is introduced and its CDF, PDF, HF, SF, and CHF are derived. Section III introduces the NU-Weibull distribution. Section IV provides the distributional properties (statistical properties) of the NU-W family. Section V offers a practical demonstration of the NU-Weibull model using engineering datasets. Finally, Sec. VI provides some final concluding remarks.

II. A NU-*W* FAMILY

Now, assume T has the NU-W family with CDF symbolized by $K(t;\alpha,\phi,\psi)$ and defined by

$$K(t;\alpha,\phi,\psi) = 1 - \left(\frac{S(t;\psi)}{\phi}\left\{\phi - [W(t;\psi)]^{\alpha}\right\}\right), \quad t \in \mathbb{R}, \tag{2}$$

where $\phi(|\phi| >= 1)$ and $\alpha(\alpha > 0)$. $S(t;\psi) = 1 - W(t;\psi)$ represents the baseline SF, and ψ is the parameter vector attached with the baseline CDF $W(t;\psi)$. It is important to note that

(i) when $\phi \geq 1$, then α can be greater than zero, i.e., $\alpha > 0$, and
(ii) when $\phi \leq -1$, then α should be greater than one, i.e., $\alpha > 1$.

Propositions 1 and 2 provide a detailed mathematical description ensuring that $K(t;\alpha,\phi,\psi)$ in Eq. (2) is a valid CDF.

Proposition 1. For $K(t;\alpha,\phi,\psi)$ in Eq. (2), we need to prove

$$\lim_{t\to-\infty} K(t;\alpha,\phi,\psi) = 0,$$

and

$$\lim_{t\to\infty} K(t;\alpha,\phi,\psi) = 1.$$

Proof. From Eq. (2), we have

$$K(t;\alpha,\phi,\psi) = 1 - \left(\frac{S(t;\psi)}{\phi}\left\{\phi - [W(t;\psi)]^{\alpha}\right\}\right). \tag{3}$$

Applying $\lim_{t\to-\infty}$ to both sides of Eq. (3), we get

$$\lim_{t\to-\infty} K(t;\alpha,\phi,\psi) = \left(1 - \left(\frac{S(-\infty;\psi)}{\phi}\left\{\phi - [W(-\infty;\psi)]^{\alpha}\right\}\right)\right). \tag{4}$$

Since $W(t;\psi)$ is a valid CDF and $S(t;\psi)$ is a valid SF. So, we have

$$\lim_{t\to-\infty} W(t;\psi) = 0,$$

and

$$\lim_{t\to-\infty} S(t;\psi) = S(-\infty;\psi) = 1.$$

Thus, from Eq. (4), we have

$$\lim_{t\to-\infty} K(t;\alpha,\phi,\psi) = 1 - \left(\frac{1}{\phi}\{\phi - 0\}\right),$$

$$\lim_{t\to-\infty} K(t;\alpha,\phi,\psi) = 0.$$

From Eq. (2), we also obtain

$$\lim_{t\to\infty} K(t;\alpha,\phi,\psi) = 1 - \left(\frac{S(\infty;\psi)}{\phi}\left\{\phi - [W(\infty;\psi)]^{\alpha}\right\}\right). \tag{5}$$

As we have already mentioned that $W(t;\psi)$ is a valid CDF and $S(t;\psi)$ is a valid SF. Then, we have

$$\lim_{t\to\infty} W(t;\psi) = 1,$$

and

$$\lim_{t\to\infty} S(t;\psi) = S(\infty;\psi) = 0.$$

Using Eq. (5), we have

$$\lim_{t\to\infty} K(t;\alpha,\phi,\psi) = 1 - \left(\frac{0}{\phi}\{\phi - 1\}\right),$$

$$\lim_{t\to\infty} K(t;\alpha,\phi,\psi) = 1.$$

Proposition 2. The CDF $K(t;\alpha,\phi,\psi)$ is differentiable.

Proof.

$$\frac{d}{dt}K(t;\alpha,\phi,\psi) = k(t;\alpha,\phi,\psi).$$

The proof of Proposition 2 is very straightforward and the derivative of $K(t;\alpha,\phi,\psi)$ (which is the PDF) is given as follows:

$$k(t;\alpha,\phi,\psi) = \frac{w(t;\psi)}{\phi}\left(\phi + \alpha[W(t;\psi)]^{\alpha-1} - (\alpha+1)[W(t;\psi)]^{\alpha}\right). \tag{6}$$

Corresponding to Eqs. (2) and (3), the SF indicated by $S(t;\alpha,\phi,\psi) = 1 - K(t;\alpha,\phi,\psi)$, HF indicated by $h(t;\alpha,\phi,\psi) = \frac{k(t;\alpha,\phi,\psi)}{S(t;\alpha,\phi,\psi))}$, and CHF indicated by $H(t;\alpha,\phi,\psi) = -\log[S(t;\alpha,\phi,\psi)]$ of the NU-W distributions can be, respectively, simplify as follows:

$$S(t;\alpha,\phi,\psi) = \left(\frac{S(t;\psi)}{\phi}\{\phi - [W(t;\psi)]^{\alpha}\}\right),$$

$$h(v;\lambda,\Xi) = \frac{w(t;\psi)\left(\phi + \alpha[W(t;\psi)]^{\alpha-1} - (\alpha+1)[W(t;\psi)]^{\alpha}\right)}{S(t;\psi)\{\phi - [W(t;\psi)]^{\alpha}\}},$$

and

$$H(t;\alpha,\phi,\psi) = -\log\left(\frac{S(t;\psi)}{\phi}\{\phi - [W(t;\psi)]^{\alpha}\}\right).$$

By using $W(t;\psi) = 1 - e^{-\sigma t^{\eta}}$ in Eq. (2), we get the CDF of the NU-Weibull distribution.

III. A NU-WEIBULL DISTRIBUTION

This section presents the mathematical backgrounds of the proposed NU-Weibull distribution. Assume T has the NU-Weibull distribution with CDF $K(t;\alpha,\phi,\psi)$ and PDF $k(t;\alpha,\phi,\psi)$ defined by

$$K(t;\alpha,\phi,\psi) = 1 - \left(\frac{e^{-\sigma t^{\eta}}}{\phi}\left\{\phi - \left[1 - e^{-\sigma t^{\eta}}\right]^{\alpha}\right\}\right), \qquad t \in \mathbb{R}, \tag{7}$$

and SF $k(t;\alpha,\phi,\psi)$ given by

$$S(t;\alpha,\phi,\psi) = \frac{e^{-\sigma t^{\eta}}}{\phi}\left\{\phi - \left[1 - e^{-\sigma t^{\eta}}\right]^{\alpha}\right\}.$$

Figures 1 and 2 display the plots of $K(t;\alpha,\phi,\psi)$ and $S(t;\alpha,\phi,\psi)$ of the NU-Weibull distribution, respectively.

The PDF $k(t;\alpha,\phi,\psi)$ of the NU-Weibull distribution is

$$k(t;\alpha,\phi,\psi) = \frac{\eta\sigma t^{\eta-1}e^{-\sigma t^{\eta}}}{\phi}\left(\phi + \alpha\left[1 - e^{-\sigma t^{\eta}}\right]^{\alpha-1} - (\alpha+1)\left[1 - e^{-\sigma t^{\eta}}\right]^{\alpha}\right). \tag{8}$$

The graphical display of $k(t;\alpha,\phi,\psi)$ is provided in Fig. 3. The plots of $k(t;\alpha,\phi,\psi)$ in Fig. 3 are provided for (*a*) $\eta = 0.5, \sigma = 1.0, \alpha = 0.5, \phi = 1.2$, (*b*) $\eta = 1.2, \sigma = 2.0, \alpha = 1.5, \phi = -1.2$, (*c*) $\eta = 2.1, \sigma = 1.0, \alpha = 0.2, \phi = 4.8$, (*d*) $\eta = 1.1, \sigma = 1.0, \alpha = 3.2, \phi = 5.4$, (*e*) $\eta = 4.9, \sigma = 0.01, \alpha = 3.2, \phi = 5.4$, and (*f*) $\eta = 5.9, \sigma = 0.009, \alpha = 0.5, \phi = 4.2$.

From Fig. 3, it is very noticeable that the NU-Weibull distribution has six different patterns of $k(t;\alpha,\phi,\psi)$ such as (*i*) decreasing shaped, (*ii*) bimodal, (*iii*) decreasing-increasing-decreasing, (*iv*) right-skewed, (*v*) left-skewed, and (*vi*) symmetrical. These plots show the flexibility of the proposed NU-Weibull distribution.

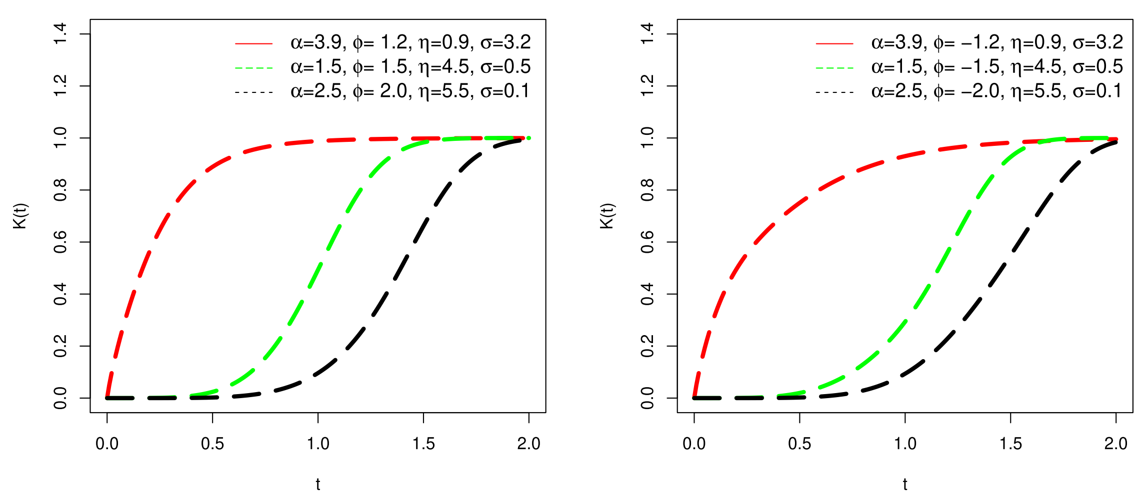

FIG. 1. Plots of $K(t;\alpha,\phi,\psi)$ of the NU-Weibull model.

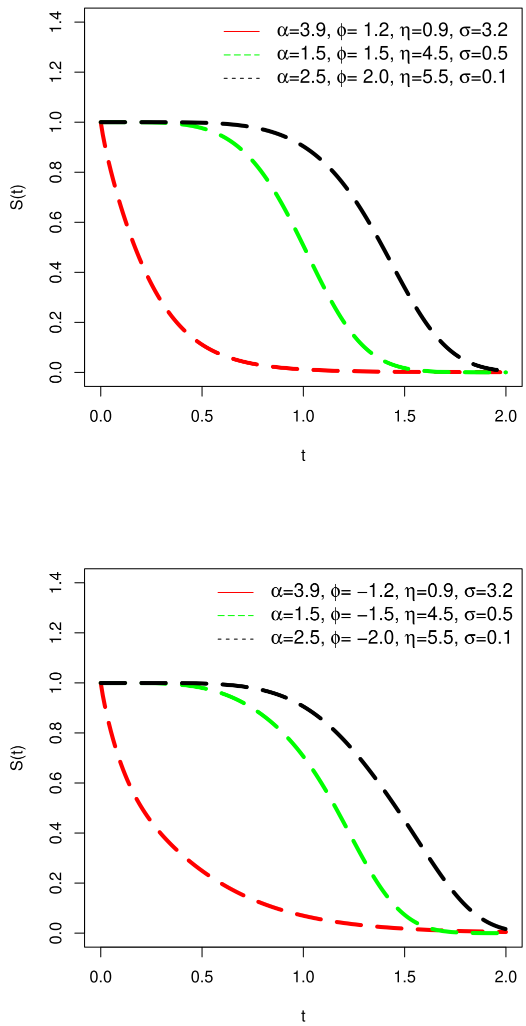

FIG. 2. Plots of $S(t;\alpha,\phi,\psi)$ of the NU-Weibull model.

In addition, the HF of the NU-Weibull distribution is

$$h(t;\alpha,\phi,\psi) = \frac{\sigma}{\left\{\phi - \left[1 - e^{-\sigma t^{\eta}}\right]^{\alpha}\right\}}\left(\phi + \alpha\left[1 - e^{-\sigma t^{\eta}}\right]^{\alpha-1} - (\alpha+1)\left[1 - e^{-\sigma t^{\eta}}\right]^{\alpha}\right),$$

and the CHF is

$$H(t;\alpha,\phi,\psi) = -\log\left(\frac{e^{-\sigma t^{\eta}}}{\phi}\left\{\phi - \left[1 - e^{-\sigma t^{\eta}}\right]^{\alpha}\right\}\right).$$

IV. DISTRIBUTIONAL PROPERTIES

In this section, we derive some useful distributional properties of the NU-W distributions such as the identifiability property (IP), quantile function (QF), heavy-tailed (HT) property, rth moment, and MGF (moment generating function).

A. The identifiability property

In distribution theory and model analysis, identifiability is a fundamental concept in the estimation of the parameters of a model (or distribution). IP helps to assess whether it is theoretically possible to find unique parameter values from a dataset given the model structure, properties of errors in the model, and so on. Note that using non-identifiable models can considerably affect the outcomes in real-world applications. This section provides the derivation of the IP of NU-W distributions using both the additional parameters α and ϕ.

1. The derivation of the IP of α

The parameter α is said to follow the IP, if $\alpha_1 = \alpha_2$.

Suppose α_1 and α_2 are two parameters with CDFs $K(t;\alpha_1,\phi,\psi)$ and $K(t;\alpha_2,\phi,\psi)$, respectively. Using the mathematical definition of the IP, we have

$$K(t;\alpha_1,\phi,\psi) = K(t;\alpha_2,\phi,\psi). \tag{9}$$

Using Eq. (2) in Eq. (9), we get

$$1 - \left(\frac{S(t;\psi)}{\phi}\left\{\phi - [W(t;\psi)]^{\alpha_1}\right\}\right) = 1 - \left(\frac{S(t;\psi)}{\phi}\left\{\phi - [W(t;\psi)]^{\alpha_2}\right\}\right),$$

$$\left(\frac{S(t;\psi)}{\phi}\left\{\phi - [W(t;\psi)]^{\alpha_1}\right\}\right) = \left(\frac{S(t;\psi)}{\phi}\left\{\phi - [W(t;\psi)]^{\alpha_2}\right\}\right),$$

$$\phi - [W(t;\psi)]^{\alpha_1} = \phi - [W(t;\psi)]^{\alpha_2},$$

$$[W(t;\psi)]^{\alpha_1} = [W(t;\psi)]^{\alpha_2},$$

$$\alpha_1 \log[W(t;\psi)] = \alpha_2 \log[W(t;\psi)],$$

$$\alpha_1 = \alpha_2.$$

2. The derivation of the IP of ϕ

The parameter ϕ is said to follow the IP, if we prove $\phi_1 = \phi_2$.

Suppose ϕ_1 and ϕ_2 have the CDFs $K(t;\alpha,\phi_1,\psi)$ and $K(t;\alpha,\phi_2,\psi)$, respectively. Again, by implementing the mathematical definition of the IP, we have

$$K(t;\alpha,\phi_1,\psi) = K(t;\alpha,\phi_2,\psi). \tag{10}$$

Using Eq. (2) in Eq. (10), we get

$$1 - \left(\frac{S(t;\psi)}{\phi_1}\left\{\phi_1 - [W(t;\psi)]^{\alpha}\right\}\right) = 1 - \left(\frac{S(t;\psi)}{\phi_2}\left\{\phi_2 - [W(t;\psi)]^{\alpha}\right\}\right),$$

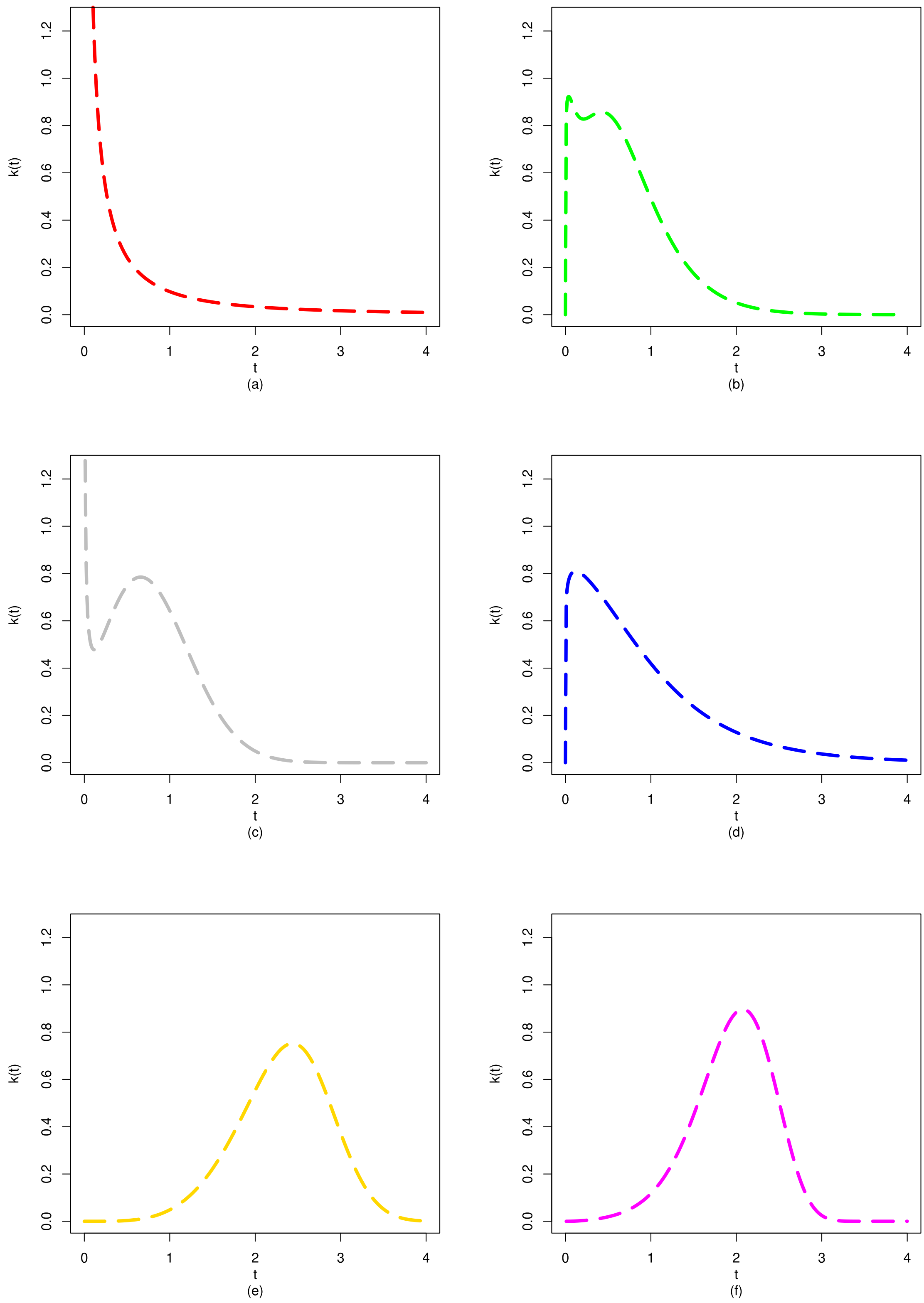

FIG. 3. Plots of $k(t;\alpha,\phi,\psi)$ of the NU-Weibull model.

$$\frac{S(t;\psi)}{\phi_1}\{\phi_1 - [W(t;\psi)]^\alpha\} = \frac{S(t;\psi)}{\phi_2}\{\phi_2 - [W(t;\psi)]^\alpha\},$$

$$\frac{1}{\phi_1}\{\phi_1 - [W(t;\psi)]^\alpha\} = \frac{1}{\phi_2}\{\phi_2 - [W(t;\psi)]^\alpha\},$$

$$\phi_2\{\phi_1 - [W(t;\psi)]^\alpha\} = \phi_1\{\phi_2 - [W(t;\psi)]^\alpha\},$$

$$\phi_1\phi_2 - \phi_2[W(t;\psi)]^\alpha = \phi_1\phi_2 - \phi_1[W(t;\psi)]^\alpha,$$

$$\phi_2[W(t;\psi)]^\alpha = \phi_1[W(t;\psi)]^\alpha,$$

$$\phi_1 = \phi_2.$$

B. The HT property

Among the classes of probability distributions, those that possess the HT properties are very useful for dealing with real phenomena (or real-life data) extreme value data. A probability model is termed an HT model, if its SF $S(t;\alpha,\phi,\psi)$ satisfies the following:

$$\lim_{t\to\infty} e^{qt} S(t;\alpha,\phi,\psi) = \infty,$$

where $q > 0$.

The HT probability distributions possess a very useful characteristic called the RVar (regular variational) property. A statistical model is said to be an RVar model, if it satisfies

$$\lim_{t\to\infty} \frac{S(zt;\alpha,\phi,\psi)}{S(t;\alpha,\phi,\psi)} = z^\lambda, \quad \lambda > 0, z > 0.$$

For more details on HT distributions, see Refs. 29–31.

This section provides the proof of the RVar characteristic of the NU-W distributions. Following the approach of Ref. 32, using the SF $S(.)$, we have

Theorem. If $S(t;\psi) = 1 - W(t;\psi)$ is a RVar model, then $S(t;\alpha,\phi,\psi) = 1 - K(t;\alpha,\phi,\psi)$ is also a RVar model.

Proof. Assume that $\lim_{t\to\infty} \frac{S(zt;\psi)}{S(t;\psi)} = g(z)$ is finite but nonzero $\forall\ z > 0$. Using Eq. (2), we have

$$\lim_{t\to\infty} \frac{S(zt;\alpha,\phi,\psi)}{S(t;\alpha,\phi,\psi)} = \lim_{t\to\infty} \frac{\left(\frac{S(zt;\psi)}{\phi}\{\phi - [W(zt;\psi)]^\alpha\}\right)}{\left(\frac{S(t;\psi)}{\phi}\{\phi - [W(t;\psi)]^\alpha\}\right)}$$

$$= \lim_{t\to\infty} \frac{S(zt;\psi)}{S(t;\psi)} \times \lim_{t\to\infty} \frac{\{\phi - [W(zt;\psi)]^\alpha\}}{\{\phi - [W(t;\psi)]^\alpha\}}$$

$$= \lim_{t\to\infty} \frac{S(zt;\psi)}{S(t;\psi)} \times \lim_{t\to\infty} \frac{\{\phi - [W(zt;\psi)]^\alpha\}}{\{\phi - [W(t;\psi)]^\alpha\}}. \quad (11)$$

Using $W(t;\psi) = 1 - e^{-\sigma t^\eta}$ and $W(zt;\psi) = 1 - e^{-\sigma(zt)^\eta}$ in Eq. (11), we get

$$\lim_{t\to\infty} \frac{S(zt;\alpha,\phi,\psi)}{S(t;\alpha,\phi,\psi)} = \lim_{t\to\infty} \frac{S(zt;\psi)}{S(t;\psi)} \times \lim_{t\to\infty} \frac{\left\{\phi - \left[1 - e^{-\sigma(zt)^\eta}\right]^\alpha\right\}}{\left\{\phi - \left[1 - e^{-\sigma t^\eta}\right]^\alpha\right\}}$$

$$= \lim_{t\to\infty} \frac{S(zt;\psi)}{S(t;\psi)} \times \frac{\left\{\phi - \left[1 - e^{-\sigma(z\times\infty)^\eta}\right]^\alpha\right\}}{\left\{\phi - \left[1 - e^{-\sigma(\infty)^\eta}\right]^\alpha\right\}}$$

$$= \lim_{t\to\infty} \frac{S(zt;\psi)}{S(t;\psi)} \times \frac{\{\phi - [1 - e^{-\infty}]^\alpha\}}{\{\phi - [1 - e^{-\infty}]^\alpha\}}$$

$$= \lim_{t\to\infty} \frac{S(zt;\psi)}{S(t;\psi)} \times \frac{\{\phi - [1 - 0]^\alpha\}}{\{\phi - [1 - 0]^\alpha\}}$$

$$= \lim_{t\to\infty} \frac{S(zt;\psi)}{S(t;\psi)} \times \frac{\phi}{\phi}$$

$$= \lim_{t\to\infty} \frac{S(zt;\psi)}{S(t;\psi)}$$

$$= g(z).$$

C. A practical application

Consider the probability distribution of T assumes the power-law (PL) characteristic, then

$$S(t,\psi) = \mathbb{P}(T > t) \approx t^{-\mu}. \quad (12)$$

The term $S(t,\psi)$ can also be expressed as

$$S(t;\alpha,\phi,\psi) = t^{-\mu}\xi(t;\alpha,\phi,\psi),$$

where $\xi(t;\psi)$ represents the slowly varying (SVar) function. Using Eq. (2), we observe

$$S(t;\alpha,\phi,\psi) = \frac{S(t;\psi)}{\phi}\{\phi - [W(t;\psi)]^\alpha\}. \quad (13)$$

As we have, $S(t,\psi) \approx t^{-\mu}$. Therefore, Eq. (13) becomes

$$S(t;\alpha,\phi,\psi) = \frac{t^{-\mu}}{\phi}\{\phi - [1 - t^{-\mu}]^\alpha\}.$$

Let

$$S(t;\alpha,\phi,\psi) = t^{-\mu}\xi(t;\alpha,\phi,\psi),$$

where

$$\xi(t;\alpha,\phi,\psi) = \frac{1}{\phi}\{\phi - [1 - t^{-\mu}]^\alpha\}. \quad (14)$$

To prove that the NU-Weibull distribution is an RVar model, then, we must show that $\xi(t;\alpha,\phi,\psi)$ is an SVar function. The expression $\xi(t;\alpha,\phi,\psi)$ is an SVar function, if and only if, we have

$$\lim_{t\to\infty} \frac{\xi(\psi t;\alpha,\phi,\psi)}{\xi(t;\alpha,\phi,\psi)} = 1.$$

Using Eq. (14), we get

$$\frac{\xi(\psi t;\alpha,\phi,\psi)}{\xi(t;\alpha,\phi,\psi)}=\frac{\phi-\left[1-(\psi t)^{-\mu}\right]^{\alpha}}{\phi-\left[1-t^{-\mu}\right]^{\alpha}}.$$

Thus,

$$\frac{\xi(\psi t;\alpha,\phi,\psi)}{\xi(t;\alpha,\phi,\psi)}=\frac{\phi-\left[1-\frac{1}{(\psi t)^{\mu}}\right]^{\alpha}}{\phi-\left[1-\frac{1}{t^{\mu}}\right]^{\alpha}}. \tag{15}$$

By applying $\lim_{t\to\infty}$ to Eq. (15), we get

$$\begin{aligned}\lim_{t\to\infty}\frac{\xi(\psi t;\alpha,\phi,\psi)}{\xi(t;\alpha,\phi,\psi)}&=\lim_{t\to\infty}\frac{\phi-\left[1-\frac{1}{(\psi t)^{\mu}}\right]^{\alpha}}{\phi-\left[1-\frac{1}{t^{\mu}}\right]^{\alpha}}\\&=\frac{\phi-[1-0]^{\alpha}}{\phi-[1-0]^{\alpha}}\\&=\frac{\phi-1}{\phi-1}.\end{aligned}$$

Therefore,

$$\lim_{t\to\infty}\frac{\xi(\psi t;\alpha,\phi,\psi)}{\xi(t;\alpha,\phi,\psi)}=1.$$

D. The quantile function

The QF of the NU-W distributions with DF $K(t;\alpha,\phi,\psi)$ is

$$t=Q(u)=K^{-1}(u)=W^{-1}(y), \tag{16}$$

where $u\in(0,1)$ and y is the solution of $(1-y)[\phi-y^{\alpha}]-\phi(1-u)$. The QF in Eq. (16) can be used to generate RNs (random numbers) or RSs (random samples) from any special case of the NU-W family.

E. The rth moment

Here, we derive the rth moment of the NU-W family. Assume T have the NU-W family of distributions with PDF $k(t;\alpha,\phi,\psi)$ in Eq. (3), its rth moment is derived as

$$\mu_r'=\int_{\Omega}t^r\,k(t;\alpha,\phi,\psi)dt. \tag{17}$$

Using Eq. (3) in Eq. (17), we get

$$\mu_r'=\int_{\Omega}t^r\frac{w(t;\psi)}{\phi}\left(\phi+\alpha[W(t;\psi)]^{\alpha-1}-(\alpha+1)[W(t;\psi)]^{\alpha}\right)dt,$$

$$\mu_r'=\frac{\alpha}{\phi}\int_{\Omega}t^r w(t;\psi)[W(t;\psi)]^{\alpha-1}dt-\frac{(\alpha+1)}{\phi}\times\int_{\Omega}t^r w(t;\psi)[W(t;\psi)]^{\alpha}dt+\int_{\Omega}t^r w(t;\psi)dt,$$

$$\mu_r'=\frac{\alpha}{\phi}\int_{\Omega}t^r w(t;\psi)[W(t;\psi)]^{\alpha-1}dt-\frac{(\alpha+1)}{\phi}\times\int_{\Omega}t^r w(t;\psi)[W(t;\psi)]^{(\alpha+1)-1}dt+\int_{\Omega}t^r w(t;\psi)dt,$$

$$\mu_r'=\int_{\Omega}t^r\left(\frac{1}{\phi}g_1(t;\psi)-\frac{1}{\phi}g_2(t;\psi)+w(t;\psi)\right)dt,$$

where

$$g_1(t;\psi)=\alpha w(t;\psi)[W(t;\psi)]^{\alpha-1},$$

and

$$g_2(t;\psi)=(\alpha+1)w(t;\psi)[W(t;\psi)]^{(\alpha+1)-1}.$$

V. RESIDUAL LIFE ANALYSIS OF THE NU-WEIBULL DISTRIBUTION

In Ref. 33, the authors devolved a class of aging distributions having decreasing variance residual life. In Ref. 34, it is shown that the variance and coefficient of variation of residual life are closely related to the mean residual life's behavior of the induced distribution. The mean of the random residual life is also termed the mean residual life at age t. Thus, the mean residual life (MRL) is a function of age t. Therefore, it is also referred to as the MRL function (MRLF). Many researchers have advocated that residual life properties are very important in the analysis of lifetime data and failure time of electronic devices in reliability studies; see, for instance, Ref. 35. In this section, we discuss the properties of the residual life function (RLF) of the proposed NU-Weibull distribution.

Let assume that T is a continuous positive random variable with absolutely continuous distribution function $K(t;\alpha,\phi,\psi)$ with the corresponding SF $\bar{K}(t;\alpha,\phi,\psi)=1-K(t;\alpha,\phi,\psi)$, where $K(0;\alpha,\phi,\psi)=1$. Then, the MRLF is given by

$$\mu_K(t;\alpha,\phi,\psi)=E(X-t|X>t)=\frac{1}{\bar{K}(t;\alpha,\phi,\psi)}\times\int_t^{\infty}\bar{K}(x;\alpha,\phi,\psi)dx,\quad t\geq 0. \tag{18}$$

The variance RLF (VRLF) is

$$\sigma_K^2(t;\alpha,\phi,\psi)=\frac{2}{\bar{K}(t;\alpha,\phi,\psi)}\int_t^{\infty}\int_x^{\infty}\bar{K}(y;\alpha,\phi,\psi)dy\,dx-\mu_K^2(t;\alpha,\phi,\psi). \tag{19}$$

The coefficient of variation of the RLF (CVRLF) is

$$\varsigma_K=\frac{\sigma_K(t;\alpha,\phi,\psi)}{\mu_K(t;\alpha,\phi,\psi)},$$

where $\mu_K(0;\alpha,\phi,\psi)=0$.

Figure 4 displays the MRLF of the proposed NU-Weibull distribution using the parameters introduced in Sec. III. From Fig. 4(a), it can be seen that the MRLF is an increasing function when $(\eta,\sigma,\alpha,\phi,\psi)=(0.5,1.0,0.5,1.2)$. In Figs. 4(b) and 4(c), it can be seen that when $(\eta,\sigma,\alpha,\phi,\psi)=(1.2,2.0,1.5,-1.2)$ and $(\eta,\sigma,\alpha,\phi,\psi)=(2.1,1.0,0.2,4.8)$, the MRLF is asymptotic to the *x-axis* and an *oblique* line, respectively. Figure 4(d) shows that the MRLF is decreasing when $t<18$ and increasing when $t>18$ for $(\eta,\sigma,\alpha,\phi,\psi)=(1.1,1.0,3.2,5.4)$. From Fig. 4(e), it can be seen that the MRLF is a decreasing function when $(\eta,\sigma,\alpha,\phi,\psi)=(4.9,0.01,3.2,5.4)$. Figure 4(f) shows that the MRLF is decreasing when $t<25$ and asymptotic to the *x-axis* when $t>25$ for $(\eta,\sigma,\alpha,\phi,\psi)=(5.9,0.009,0.5,4.24)$.

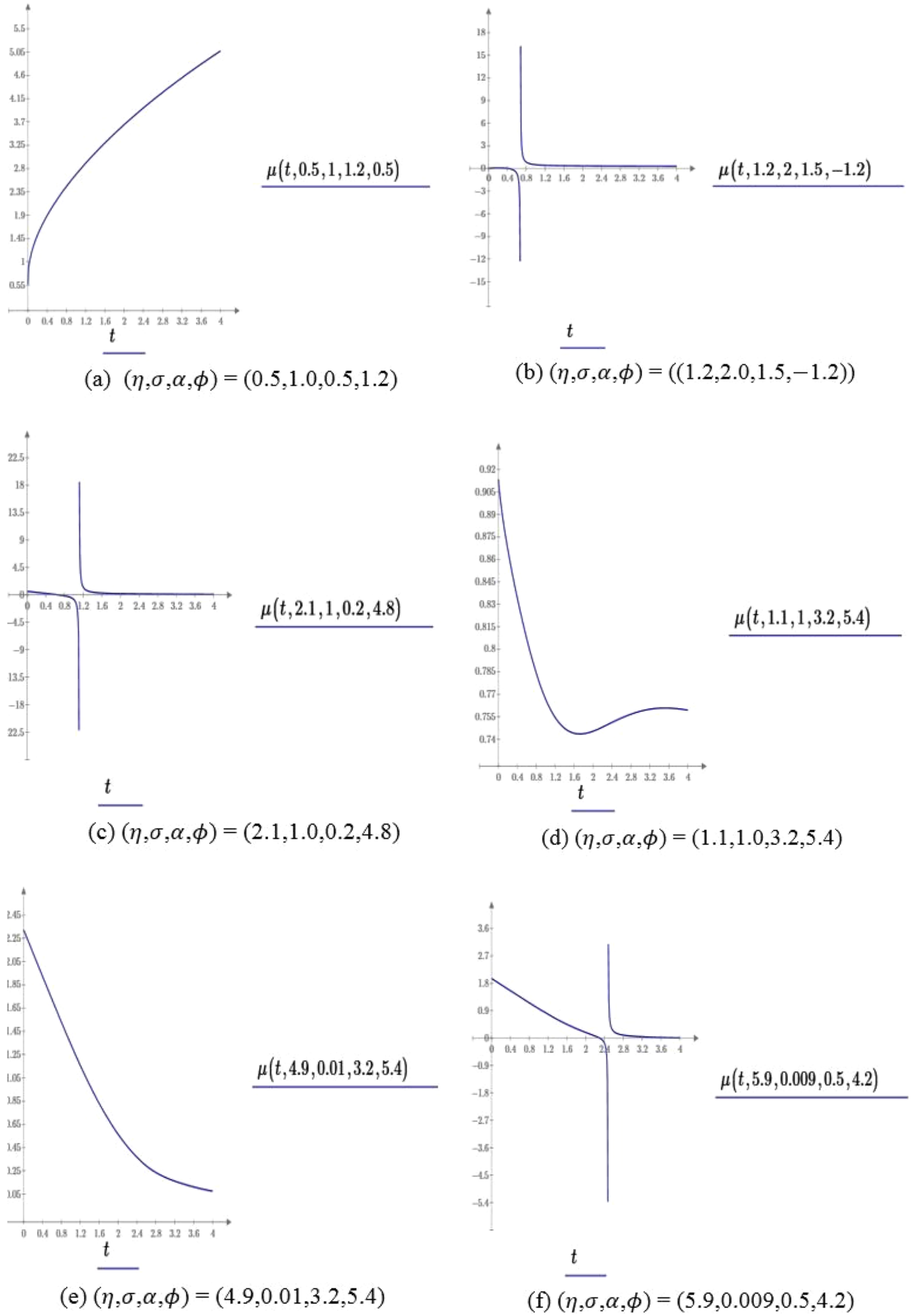

FIG. 4. Mean residual life function (MRLF) for six different shapes of the NU-Weibull function.

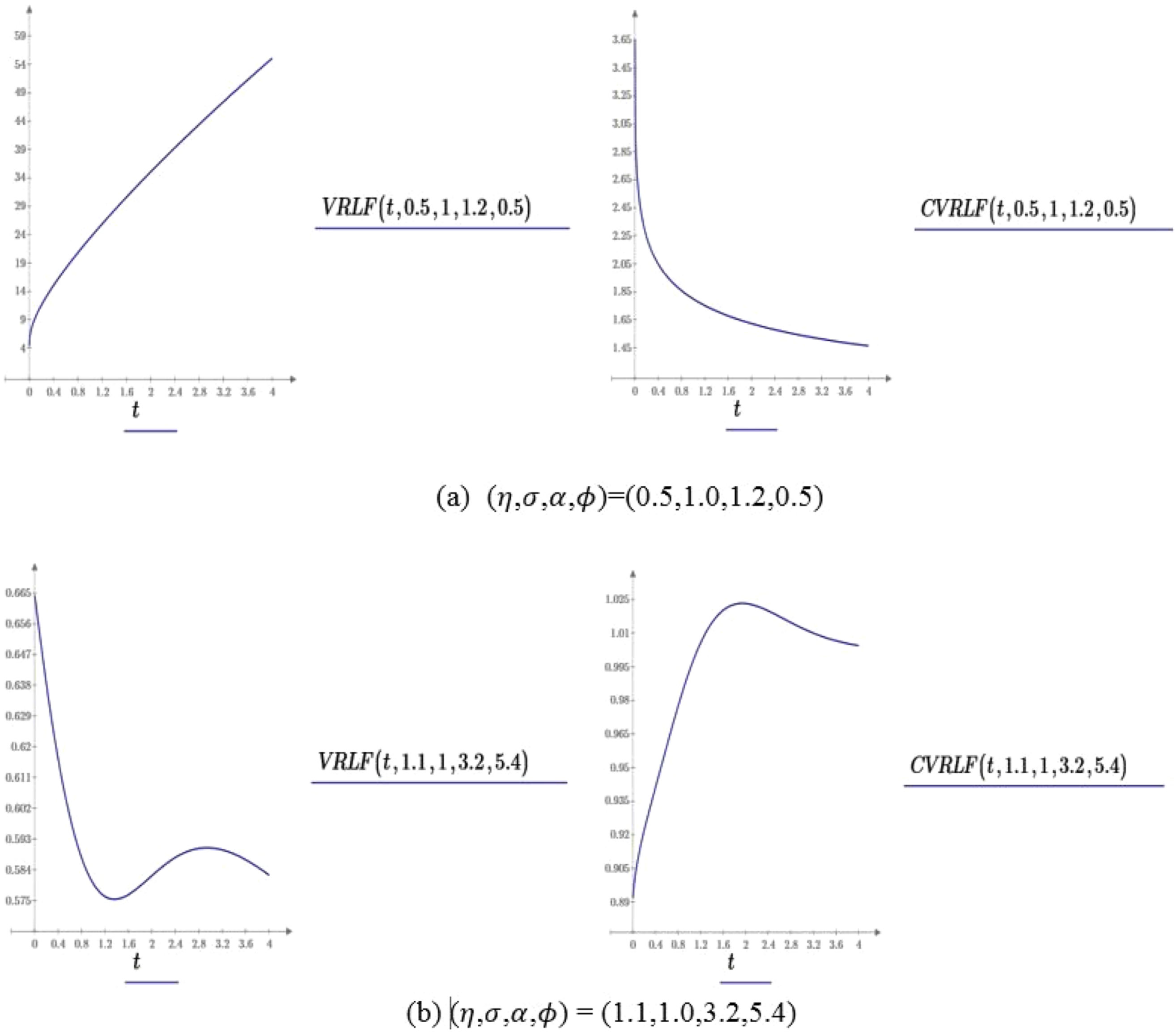

FIG. 5. VRLF and CVRLF for two different shapes of the NU-Weibull function.

Figure 5 displays the VRLF and CVRLF of the proposed NU-Weibull distribution when $(\eta, \sigma, \alpha, \phi, \psi) = (1.1, 1.0, 3.2, 5.4)$ and $(\eta, \sigma, \alpha, \phi, \psi) = (0.5, 1.0, 1.2, 0.5)$. This figure depicts the connection between the VRLF and CVRLF. It can be seen that as the CRLF decreases (increases), the VRLF increases (decreases).

VI. DATA ANALYSES

We present two real-world engineering datasets on account to illustrate the application and effectiveness of the NU-Weibull model. The first illustration of the NU-Weibull model is performed using a dataset from civil engineering. The second illustration of the NU-Weibull model is carried out using lifetime data taken from the reliability sector.

We apply the NU-Weibull model to both the civil engineering and reliability engineering data and compare its fitting power (or numerical results) with the ones of the existing Weibull model, the Kumaraswamy Weibull (K-Weibull), and the exponentiated Weibull (E-Weibull) models. The CDFs of the E-Weibull and K-Weibull models are given by

$$K(t;\theta_1,\psi) = \left(1 - e^{-\sigma t^{\eta}}\right)^{\theta_1}, \qquad t \geq 0,$$

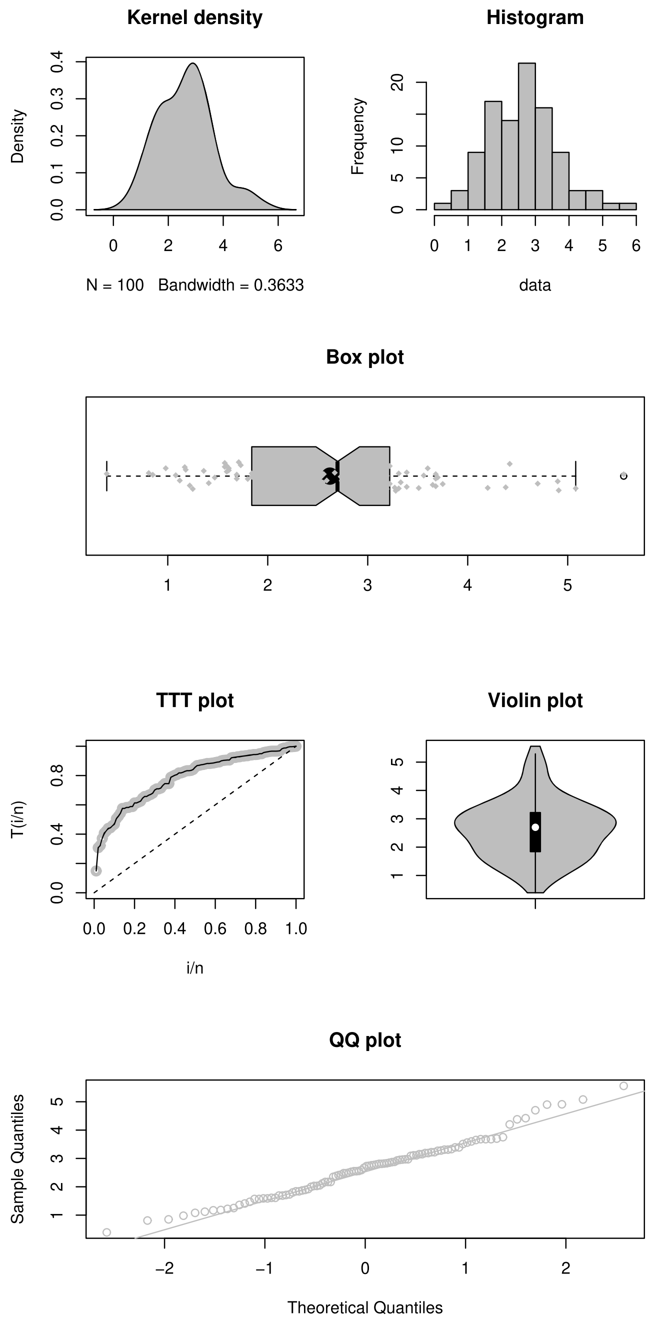

FIG. 6. Descriptive plots of the carbon fibers data.

and

$$K(t;\theta_1,\theta_2,\psi) = 1 - \left[1 - \left(1 - e^{-\sigma t^{\eta}}\right)^{\theta_1}\right]^{\theta_2}, \qquad t \geq 0,$$

respectively, where $\theta_1 > 0, \theta_2 > 0, \sigma > 0, \eta > 0$.

After choosing two different variants of the Weibull model as competing distributions, now, we go for certain analytical/evaluation measures to identify the more suitable model among the NU-Weibull and other different variants of the Weibull model. These analytical quantities include the (*a*) Cramér-von Mises (CM) test, (*b*) Anderson Darling (AD) test, (*c*) Kolmogorov–Smirnov (KS) test, and a *p-value* associated with the KS test. The values of these above-mentioned tests are, respectively, obtained as

$$-\frac{1}{m}\sum_{v=1}^{m}(2v-1)[\log K(t_v) + \log\{1 - K(t_{m-v+1})\}] - m,$$

$$\sum_{v=1}^{m}\left[\frac{2v-1}{2m} - K(t_v)\right]^2 + \frac{1}{12m},$$

and

$$\sup_{v}[K_v(t) - K(t)],$$

respectively.

A. Illustrative example using civil engineering dataset

In this section, we provide the first illustration of the implementation of the NU-Weibull model using a civil engineering dataset. This dataset represents the breaking stress of carbon fibers. It can be found in Refs. 35 and 36. This dataset is also given by 5.56, 5.08, 4.91, 4.90, 4.70, 4.42, 4.38, 4.20, 3.75, 3.70, 3.68, 3.68, 3.68, 3.65, 3.60, 3.56, 3.51, 3.39, 3.39, 3.33, 3.31, 3.31, 3.28, 3.27, 3.22, 3.22, 3.19, 3.19, 3.15, 3.15, 3.11, 3.11, 3.09, 2.97, 2.97, 2.96, 2.95, 2.93, 2.88, 2.87, 2.85, 2.83, 2.82, 2.81, 2.81, 2.79, 2.77, 2.76, 2.74, 2.73, 2.67, 2.59, 2.56, 2.55, 2.55, 2.53, 2.50, 2.48, 2.48, 2.43, 2.41, 2.38, 2.35, 2.17, 2.17, 2.17, 2.12, 2.05, 2.03, 2.03, 2.00, 1.92, 1.89, 1.87, 1.84, 1.84, 1.80, 1.73, 1.71, 1.69, 1.69, 1.61, 1.61, 1.59, 1.59, 1.57, 1.57, 1.47, 1.41, 1.36, 1.25, 1.22, 1.18, 1.17, 1.12, 1.08, 0.98, 0.85, 0.81, 0.39.

The key measures of the carbon fiber data are kurtosis = 3.104 939, maximum = 5.560, median = 2.700, minimum = 0.390, first quartile = 1.840, third quartile = 3.220, variance = 1.027 964, skewness = 0.368 154 1, mean (or $\bar{t}$) = 2.621, and range = 5.17. Using the carbon fiber data, the known basic plots are put on view in Fig. 6.

TABLE I. The values of $\hat{\eta}_{MLE}, \hat{\sigma}_{MLE}, \hat{\alpha}_{MLE}, \hat{\phi}_{MLE}, \hat{\theta}_{1MLE}$, and $\hat{\theta}_{2MLE}$ for the carbon fibers data.

Models	$\hat{\eta}_{MLE}$	$\hat{\sigma}_{MLE}$	$\hat{\alpha}_{MLE}$	$\hat{\phi}_{MLE}$	$\hat{\theta}_{1MLE}$	$\hat{\theta}_{2MLE}$
NU-Weibull	2.7214	0.0485	2.8996	2.4785	...	...
Weibull	2.7962	0.0485	...	...	...	...
E-Weibull	2.2918	0.1125	...	...	1.4147	...
K-Weibull	2.1270	0.0973	...	...	1.5284	1.5894

TABLE II. The empirical results of the fitted models for the carbon fibers data.

Models	CM	AD	KS	*p-value*
NU-Weibull	0.0532	0.3576	0.0546	0.9265
Weibull	0.0623	0.4160	0.0623	0.8264
E-Weibull	0.0746	0.4236	0.0733	0.6553
K-Weibull	0.0760	0.4260	0.0719	0.6801

The MLEs $\hat{\eta}_{MLE}, \hat{\sigma}_{MLE}, \hat{\alpha}_{MLE}, \hat{\phi}_{MLE}, \hat{\theta}_{1MLE}$, and $\hat{\theta}_{2MLE}$ of the NU-Weibull model and other probability models using the carbon fibers data are presumed in Table I.

The numerical results of the diagnostic performances of the fitted distributions are accorded in Table II. The numerical findings of this study confirm the suitability (close-fitting) of the NU-Weibull model for the carbon fibers data (see Table II).

After showing the suitability of the NU-Weibull model numerically, we also consider a graphical approach for proving the suitability of the NU-Weibull model; see Fig. 7. For the purpose of the graphical illustration of the NU-Weibull model, we consider the estimated plots along with the PP, and QQ functions; see Fig. 7. These plots are obtained using the following expressions:

$$k(t;\alpha,\phi,\psi) = \frac{2.721\,378 \times 0.048\,408 t^{1.721\,378} e^{-0.048\,408 t^{2.721\,378}}}{2.478\,453 \times \left(2.478\,453 + 2.899\,581\left[1 - e^{-0.048\,408 t^{2.721\,378}}\right]^{1.899\,581} - 3.899\,581\left[1 - e^{-0.048\,408 t^{2.721\,378}}\right]^{2.899\,581}\right)},$$

$$K(t;\hat{\alpha},\hat{\phi},\hat{\psi}) = 1 - \frac{e^{-0.048\,408 t^{2.721\,378}}}{2.478\,453}\left\{2.478\,453 - \left[1 - e^{-0.048\,408 t^{2.721\,378}}\right]^{2.899\,581}\right\},$$

$$S(t;\hat{\alpha},\hat{\phi},\hat{\psi}) = \frac{e^{-0.048\,408 t^{2.721\,378}}}{2.478\,453 \times \left\{2.478\,453 - \left[1 - e^{-0.048\,408 t^{2.721\,378}}\right]^{2.899\,581}\right\}},$$

$$h(t;\alpha,\phi,\psi) = \frac{0.048\,408}{\left\{2.478\,453 - \left[1 - e^{-0.048\,408 t^{2.721\,378}}\right]^{1.899\,581}\right\}}\left(2.478\,453 + 2.899\,581\left[1 - e^{-0.048\,408 t^{2.721\,378}}\right]^{1.899\,581} - 3.899\,581\left[1 - e^{-0.048\,408 t^{2.721\,378}}\right]^{2.899\,581}\right),$$

and

$$H(t;\hat{\alpha},\hat{\phi},\hat{\psi}) = -\log\left(\frac{e^{-0.048\,408 t^{2.721\,378}}}{2.478\,453}\right)\left\{2.478\,453 - \left[1 - e^{-0.048\,408 t^{2.721\,378}}\right]^{2.899\,581}\right\}.$$

B. Illustrative example using engineering dataset

This section is reserved for the second illustration of the NU-Weibull distribution. We provide the second illustration of the NU-Weibull model through a dataset from reliability engineering. This dataset represents the failure time of electronic devices and can be found in Refs. 37 and 38. For interested readers, this dataset is also provided by 7.89, 4.69, 4.20, 3.34, 3.03, 3.03, 2.33, 2.17, 2.14, 2.05, 2.02, 1.81, 1.80, 1.80, 1.64, 1.63, 1.60, 1.58, 1.55, 1.54, 1.54, 1.53, 1.52, 1.51, 1.50, 1.45, 1.43, 1.40, 1.34, 1.33, 1.31, 1.29, 1.20, 1.18, 1.15, 1.11, 1.10, 1.10, 1.05, 1.03, 1.02, 1.01, 1.00, 0.99, 0.95, 0.92, 0.90, 0.85, 0.83, 0.80, 0.80, 0.79, 0.79, 0.73, 0.72, 0.72, 0.72, 0.68, 0.67, 0.65, 0.63, 0.60, 0.60, 0.56, 0.54, 0.52, 0.43, 0.42, 0.40, 0.38, 0.36, 0.35, 0.34, 0.29, 0.24, 0.24, 0.23, 0.20, 0.19, 0.18, 0.13, 0.12, 0.11, 0.11, 0.10, 0.10, 0.09, 0.09, 0.08, 0.07, 0.07, 0.06, 0.05, 0.04, 0.03, 0.03, 0.02, 0.02, 0.02, 0.01, 0.01.

The key measures of the reliability data are kurtosis = 16.708 99, maximum = 7.890 00, median = 0.800 00, minimum = 0.010 00, first quartile = 0.240 00, third quartile = 1.450 00, variance = 1.252 985, skewness = 3.001 719, mean (or $\bar{t}$) = 1.025 00, and range = 7.880 00. Using the reliability engineering data, some plots are put on view in Fig. 8.

Using the engineering data, the values of $\hat{\eta}_{MLE}, \hat{\sigma}_{MLE}, \hat{\alpha}_{MLE}, \hat{\phi}_{MLE}, \hat{\theta}_{1MLE}$, and $\hat{\theta}_{2MLE}$ of the fitted models are presumed numerically in Table III. The numerical results of the diagnostic performances of the fitted distributions are accorded in Table IV. The numerical findings of this study disclose the suitability of the NU-Weibull model for the reliability engineering data (see Table IV).

After performing the numerical illustration of the NU-Weibull model in Table IV, now, we show its best-fitting capability by considering the fitted plots along with the PP and QQ functions; see Fig. 9. These plots visually confirm the suitability of the NU-Weibull model for the reliability engineering data. For the visual illustration of the NU-Weibull model, the plots of the above quantities are sketched using the following expressions:

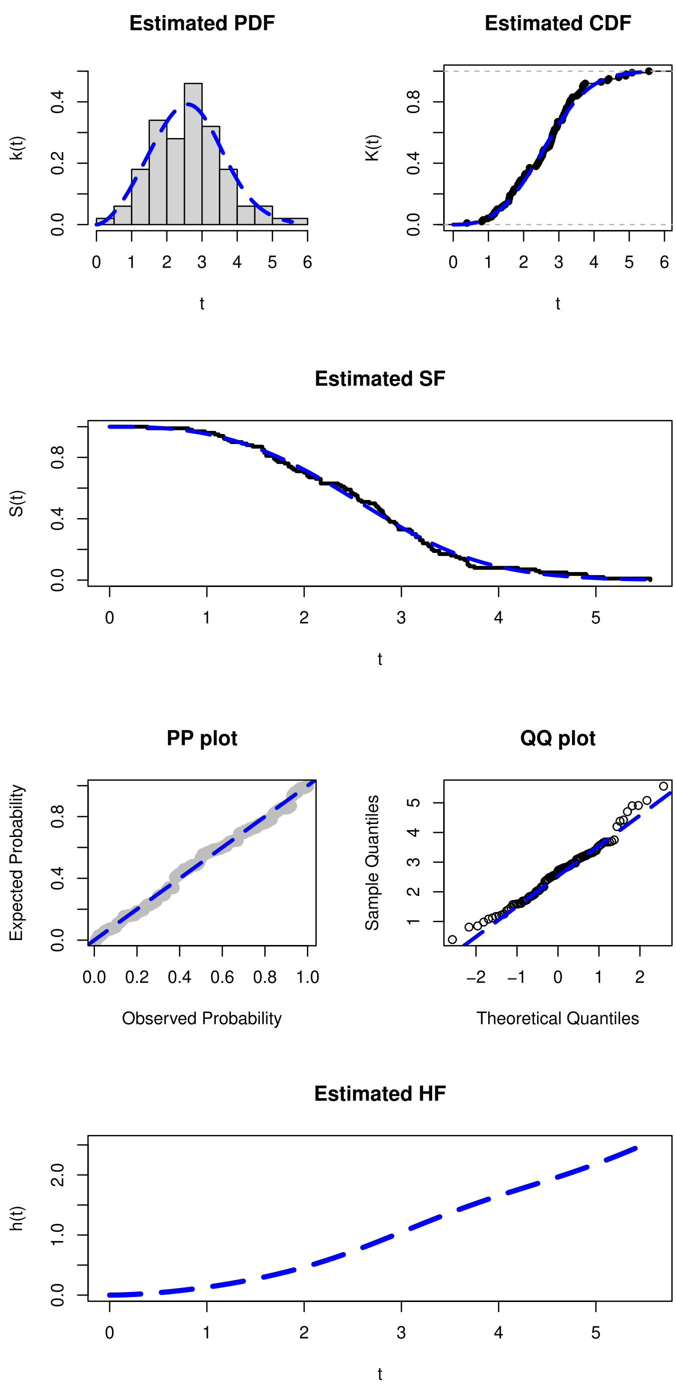

FIG. 7. The fitted and empirical plots of the NU-Weibull distribution for the carbon fibers data.

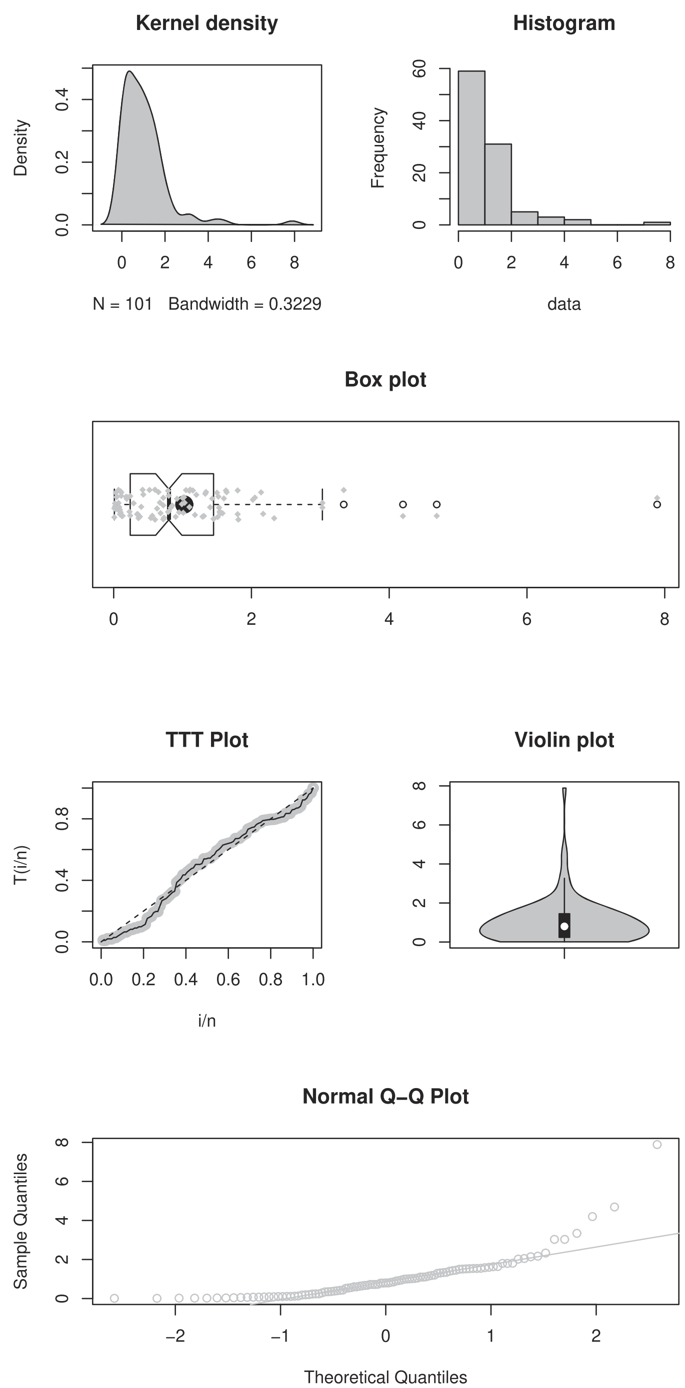

FIG. 8. Descriptive plots of the reliability data.

TABLE III. The values of $\hat{\eta}_{MLE}$, $\hat{\sigma}_{MLE}$, $\hat{\alpha}_{MLE}$, $\hat{\phi}_{MLE}$, $\hat{\theta}_{1MLE}$, and $\hat{\theta}_{2MLE}$ for the reliability data.

Models	$\hat{\eta}_{MLE}$	$\hat{\sigma}_{MLE}$	$\hat{\alpha}_{MLE}$	$\hat{\phi}_{MLE}$	$\hat{\theta}_{1MLE}$	$\hat{\theta}_{2MLE}$
NU-Weibull	0.8613	0.9043	4.3492	1.2865	⋯	⋯
Weibull	0.9256	1.0096	⋯	⋯	⋯	⋯
E-Weibull	1.0349	0.8432	⋯	⋯	0.8144	⋯
K-Weibull	1.0978	0.0995	⋯	⋯	0.8012	6.2696

TABLE IV. The empirical results of the fitted models for the reliability data.

Models	CM	AD	KS	*p-value*
NU-Weibull	0.130 60930	0.768 6836	0.077 615	0.577 000
Weibull	0.198 71740	1.111 3870	0.090 769	0.376 100
E-Weibull	0.170 12410	0.980 1112	0.089 807	0.389 200
K-Weibull	0.187 18780	1.058 5110	0.100 870	0.255 600

$$k\left(t;\hat{\alpha},\hat{\phi},\hat{\psi}\right) = \frac{0.861\,281\,6 \times 0.904\,306\,6t^{0.861\,281\,6-1}e^{-0.904\,306\,6t^{0.861\,281\,6}}}{1.286\,529\,4} \times \Bigg(1.286\,529\,4 + 4.349\,211\,7 \times \left[1-e^{-0.904\,306\,6t^{0.861\,281\,6}}\right]^{3.349\,211\,7} - 5.349\,211\,7\left[1-e^{-0.904\,306\,6t^{0.861\,281\,6}}\right]^{4.349\,211\,7}\Bigg),$$

$$S\left(t;\hat{\alpha},\hat{\phi},\hat{\psi}\right) = \frac{e^{-0.904\,306\,6t^{0.861\,281\,6}}}{1.286\,529\,4} \times \left\{1.286\,529\,4 - \left[1-e^{-0.904\,306\,6t^{0.861\,281\,6}}\right]^{4.349\,211\,7}\right\},$$

$$h\left(t;\hat{\alpha},\hat{\phi},\hat{\psi}\right) = \frac{0.904\,306\,6}{\left\{1.286\,529\,4 - \left[1-e^{-0.904\,306\,6t^{0.861\,281\,6}}\right]^{4.349\,211\,7}\right\}} \times \Bigg(1.286\,529\,4 + 4.349\,211\,7 \times \left[1-e^{-0.904\,306\,6t^{0.861\,281\,6}}\right]^{3.349\,211\,7} - 5.349\,211\,7\left[1-e^{-0.904\,306\,6t^{0.861\,281\,6}}\right]^{4.349\,211\,7}\Bigg),$$

and

$$H\left(t;\hat{\alpha},\hat{\phi},\hat{\psi}\right) = -\log\left(\frac{e^{-0.904\,306\,6t^{0.861\,281\,6}}}{1.286\,529\,4}\right) \times \left\{1.286\,529\,4 - \left[1-e^{-0.904\,306\,6t^{0.861\,281\,6}}\right]^{4.349\,211\,7}\right\}.$$

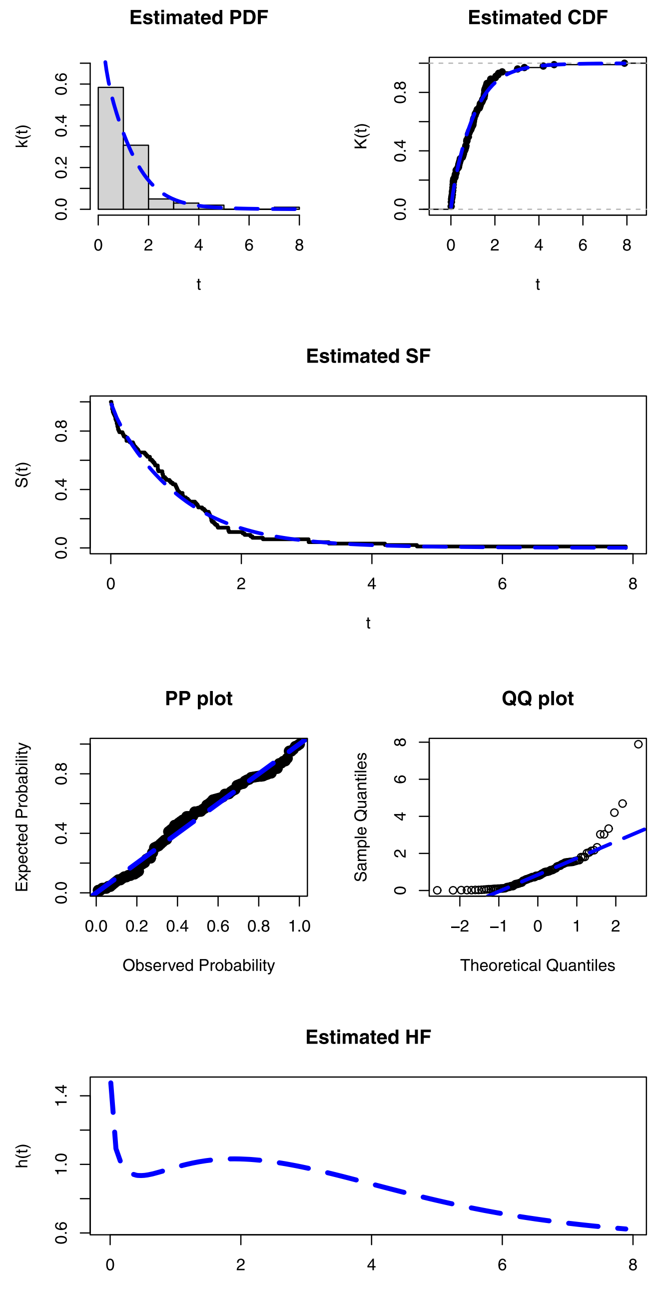

FIG. 9. The fitted and empirical plots of the NU-Weibull distribution for the reliability data.

VII. CONCLUSION

Probability models are widely used to provide the best fit to real phenomena in applied sectors. Among the applied sectors, the probability models are useful for modeling the datasets in different engineering sectors, for instance, civil, mechanical, aerospace, electrical, chemical engineering, and agricultural engineering. We proposed a novel statistical approach to generate new probability distributions for data modeling with applications in engineering sectors. The presented approach was termed a novel updated-*W* (NU-*W*) family of distributions. Corresponding to the NU-*W* method, a useful/fruitful probabilistic model, namely, a novel updated Weibull (NU-Weibull) distribution was studied. Distributional properties of NU-*W* distributions were derived. After studying the PDF of the proposed NU-Weibull distribution, it was shown that the new distribution is flexible and can take various shapes from symmetric to asymmetric distributions, and from unimodal to bimodal distribution. The residual life analysis of the NU-Weibull distribution was also provided. Finally, two data examples were considered from civil and reliability engineering to illustrate the NU-Weibull distribution. First, the NU-Weibull was applied to the civil engineering dataset, whereas the second illustration of the NU-Weibull model was carried out using a lifetime dataset. Using certain decisive criteria, it was concluded that the NU-Weibull distribution was the more suitable probability model.

ACKNOWLEDGMENTS

The researchers would like to thank the Deanship of Scientific Research, Qassim University for funding the publication of this project.

AUTHOR DECLARATIONS

Conflict of Interest

The authors have no conflicts to disclose.

Author Contributions

The authors equally contributed to the paper.

Badr Alnssyan: Formal analysis (equal). **Zubair Ahmad**: Methodology (equal). **Jean-Claude Malela-Majika**: Software (equal). **Jin-Taek Seong**: Writing – original draft (equal). **Wasswa Shafik**: Conceptualization (equal).

DATA AVAILABILITY

The datasets that support the findings of this study are provided within the article.

REFERENCES

[1] M. Bebbington, C. D. Lai, and R. Zitikis, "A flexible Weibull extension," Reliab. Eng. Syst. Saf. **92**(6), 719–726 (2007).

[2] K. Azad, M. Rasul, P. Halder, and J. Sutariya, "Assessment of wind energy prospect by Weibull distribution for prospective wind sites in Australia," Energy Procedia **160**, 348–355 (2019).

[3] M. Fidanoglu, U. Ungor, I. Ozkol, and G. Komurgoz, "Application of Weibull distribution method for aircraft component life estimation in civil aviation sector," J. Traffic Logist. Eng. **5**(1), 40–44 (2017).

[4] W. Wang, Z. Ahmad, O. Kharazmi, C. B. Ampadu, E. H. Hafez, and M. M. Mohie El-Din, "New generalized-*X* family: Modeling the reliability engineering applications," PLoS One **16**(3), e0248312 (2021).

[5] M. H. Shu, C. W. Wu, B. M. Hsu, and T. C. Wang, "Lifetime performance-qualified sampling system under a Weibull distribution with failure-censoring," Qual. Eng. **33**(3), 404–416 (2021).

[6] H. M. Khan, M. Dirikolu, and K. O. Ç. Ebubekir, "Weibull distribution of selective laser melted AlSi10Mg parts for compression testing," J. Adv. Manuf. Eng. **2**(1), 14–19 (2021).

[7] M. H. A. Hamid, M. T. Ishak, N. S. Suhaimi, J. Adnan, N. I. Hashim, M. Ariffin, N. Katim, and R. Abd Rahman, "Electrical properties of palm oil and rice bran oil under AC stress for transformer application," Alexandria Eng. J. **61**(11), 9095–9105 (2022).

[8] S. J. Almalki and J. Yuan, "A new modified Weibull distribution," Reliab. Eng. Syst. Saf. **111**, 164–170 (2013).

[9] A. Z. Afify, A. I. Shawky, and M. Nassar, "A new inverse Weibull distribution: Properties, classical and Bayesian estimation with applications," Kuwait J. Sci. **48**(3), 1–10 (2021).

[10] E. M. Almetwally, "Application of COVID-19 pandemic by using odd Lomax-G inverse Weibull distribution," Math. Sci. Lett. **10**(2), 47–57 (2021).

[11] E. Vanem and T. Fazeres-Ferradosa, "A truncated, translated Weibull distribution for shallow water sea states," Coast. Eng. **172**, 104077 (2022).

[12] T. Wang, X. He, J. Wang, and Y. Li, "Detail fatigue rating method based on bimodal Weibull distribution for DED Ti-6.5Al-2Zr-1Mo-1V titanium alloy," Chin. J. Aeronaut. **35**(4), 281–291 (2022).

[13] M. S. Rana, S. H. Shahbaz, M. Q. Shahbaz, and M. M. Rahman, "Pareto-Weibull distribution with properties and applications: A member of Pareto-X family," Pak. J. Stat. Oper. Res. **18**, 121–132 (2022).

[14] H. S. Klakattawi, "Survival analysis of cancer patients using a new extended Weibull distribution," PLoS One **17**(2), e0264229 (2022).

[15] C. Augusto-Taconeli and I. A. Rodrigues de Lara, "Discrete Weibull distribution: Different estimation methods under ranked set sampling and simple random sampling," J. Stat. Comput. Simul. **92**(8), 1740–1762 (2022).

[16] S. M. Alghamdi, R. A. R. Bantan, A. S. Hassan, H. F. Nagy, I. Elbatal, and M. Elgarhy, "Improved EDF-based tests for Weibull distribution using ranked set sampling," Mathematics **10**, 4700 (2022).

[17] S. A. Alyami, I. Elbatal, N. Alotaibi, E. M. Almetwally, H. M. Okasha, and M. Elgarhy, "Topp–Leone modified Weibull model: Theory and applications to medical and engineering data," Appl. Sci. **12**, 10431 (2022).

[18] N. Alotaibi, I. Elbatal, E. M. Almetwally, S. A. Alyami, A. S. Al-Moisheer, and M. Elgarhy, "Bivariate step-stress accelerated life tests for the Kavya–Manoharan exponentiated Weibull model under progressive censoring with applications," Symmetry **14**, 1791 (2022).

[19] N. Alotaibi, I. Elbatal, E. M. Almetwally, S. A. Alyami, A. S. Al-Moisheer, and M. Elgarhy, "Truncated Cauchy power Weibull-G class of distributions: Bayesian and non-Bayesian inference modelling for COVID-19 and carbon fiber data," Mathematics **10**, 1565 (2022).

[20] A. Abdullah Alahmadi, M. Alqawba, W. Almutiry, A. W. Shawki, S. Alrajhi, S. Al-Marzouki, and M. Elgarhy, "A new version of weighted Weibull distribution: Modelling to COVID-19 data," Discrete Dyn. Nat. Soc. **2022**, 3994361.

[21] A. S. Al-Moisheer, I. Elbatal, W. Almutiry, and M. Elgarhy, "Odd inverse power generalized Weibull generated family of distributions: Properties and applications," Math. Probl. Eng. **2021**, 5082192.

[22] A. M. Almarashi, M. Elgarhy, F. Jamal, and C. Chesneau, "The exponentiated truncated inverse Weibull-generated family of distributions with applications," Symmetry **12**, 650 (2020).

[23] S. Alkarni, A. Z. Afify, I. Elbatal, and M. Elgarhy, "The extended inverse Weibull distribution: Properties and applications," Complexity **2020**, 3297693.

[24] M. A. Aldahlan, F. Jamal, C. Chesneau, I. Elbatal, and M. Elgarhy, "Exponentiated power generalized Weibull power series family of distributions: Properties, estimation and applications," PLoS One **15**(3), e0230004 (2020).

[25] M. Elgarhy and A. Hassan, "Exponentiated weibull Weibull distribution: Statistical properties and applications," Gazi Univ. J. Sci. **32**(2), 616–635 (2019), Retrieved from https://dergipark.org.tr/en/pub/gujs/issue/45480/318297.

[26] Z. Ahmad, M. Elgarhy, and G. G. Hamedani, "A new Weibull-*X* family of distributions: Properties, characterizations and applications," J. Stat. Distrib. Appl. **5**, 5 (2018).

[27]T. H. M. Abouelmagd, S. Al-mualim, M. Elgarhy, A. Z. Afify, and M. Ahmad, "Properties of the four-parameter Weibull distribution and its applications," Pak. J. Stat. **33**, 449–466 (2017); available at http://www.pakjs.com/wp-content/uploads/2019/10/33604.pdf.

[28]Z. Ahmad, E. Mahmoudi, and G. Hamedani, "A class of claim distributions: Properties, characterizations and applications to insurance claim data," Commun. Stat.-Theory Methods **51**(7), 2183–2208 (2022).

[29]D. Bhati and S. Ravi, "On generalized log-Moyal distribution: A new heavy tailed size distribution," Insur.: Math. Econ. **79**, 247–259 (2018).

[30]Z. Li, J. Beirlant, and S. Meng, "Generalizing the log-Moyal distribution and regression models for heavy-tailed loss data," ASTIN Bull. **51**(1), 57–99 (2021).

[31]E. Seneta, "Karamata's characterization theorem, feller and regular variation in probability theory," Publ. Inst. Math. **71**(85), 79–89 (2002).

[32]R. L. Launer, "Inequalities for NBUE and NWUE life distributions," Oper. Res. **32**, 660–667 (1984).

[33]R. C. Gupta, "Variance residual life function in reliability studies," Metron-Int. J. Stat. **3**, 343–355 (2006); available at https://www.dss.uniroma1.it/RePec/mtn/articoli/2006-3-6.pdf.

[34]R. C. Gupta and S. N. U. A. Kirmani, "Some characterization of distributions by functions of failure rate and mean residual life," Commun. Stat.-Theory Methods **33**(12), 3115–3131 (2004).

[35]M. D. Nichols and W. J. Padgett, "A bootstrap control chart for Weibull percentiles," Qual. Reliab. Eng. Int. **22**(2), 141–151 (2006).

[36]J. T. Eghwerido, J. D. Ikwuoche, and O. D. Adubisi, "Inverse odd Weibull generated family of distribution," Pak. J. Stat. Oper. Res. **16**, 617–633 (2020); Eng. Int. **22**, 141–151 (2020).; available at https://doi.org/10.18187/pjsor.v16i3.2760

[37]S. Chamunorwa, B. Makubate, B. Oluyede, and F. Chipepa, "The exponentiated half logistic-log-logistic Weibull distribution: Model, properties and applications," J. Stat. Model.: Theory Appl. **2**(1), 101–120 (2021).

[38]F. Chipepa, B. Oluyede, and B. Makubate, "The odd generalized half-logistic Weibull-G family of distributions: Properties and applications," J. Stat. Model.: Theory Appl. **1**(1), 65–89 (2020); available at https://jsm.yazd.ac.ir/article_1904_50bc948d6f8f7b226e705c171b169ad2.pdf.